

Interaction between a superconducting vortex and an out-of-plane magnetized ferromagnetic disk: Influence of the magnet geometry

M. V. Milošević and F. M. Peeters*

Departement Natuurkunde, Universiteit Antwerpen (UIA), Universiteitsplein 1, B-2610 Antwerpen, Belgium

(Received 11 March 2003; revised manuscript received 29 April 2003; published 17 September 2003)

The interaction between a superconducting vortex in a type II superconducting film (SC) and a ferromagnet (FM) with out-of-plane magnetization is investigated theoretically within the London approximation. The dependence of the interaction energy on the FM-vortex distance, film thickness, and different geometries of the magnetic structures: disk, annulus (ring), square and triangle are calculated. Analytic expressions and vector-plots of the current induced in the SC due to the presence of the FM are presented. For a FM disk with a cavity, we show that different local minima for the vortex position are possible, enabling the system to be suitable to act as a qubit. For FM's with sharp edges, like e.g., for squares and triangles, the vortex prefers to enter its equilibrium position along the corners of the magnet.

DOI: 10.1103/PhysRevB.68.094510

PACS number(s): 74.78.-w, 74.25.Qt, 74.25.Ha

I. INTRODUCTION

The interaction between superconductivity and magnetism has drawn a lot of attention in the past few decades. To study the effects due to the interplay of the superconducting order parameter and the nonhomogeneous magnetic field resulting from a ferromagnet (FM), several experimental groups fabricated periodic arrays of magnetic dots and antidots positioned above or under the superconducting film.¹⁻⁴ Such ferromagnetic dots act as very effective trapping centers for the vortices which lead to an enhancement of the critical current. Recently, it was predicted⁵ that an increase of the pinning effects by two orders of magnitude can be realized in this way. After substantial progress in the preparation of regular magnetic arrays on superconductors and considering the importance of such structures for magnetic device and storage technologies, these hybrid systems became very interesting both from a theoretical and an experimental point of view. Macroscopic phenomena have already been explored experimentally, but a theoretical analysis of the magnetic and superconducting responses in such systems is still in its infancy.

In previously proposed models for the superconducting film (SC) interacting with a ferromagnet on top of it⁶⁻⁹ the magnetic texture interacts with the SC current, which subsequently changes the magnetic field. The authors used the London approximation to describe this system since the sizes of all structures are much larger than the coherence length ξ . The thickness of the SC film and of the FM was assumed to be negligibly small (i.e., $d \ll \xi, \lambda$). Elementary solutions for the interaction of the circular magnetic dot (bubble) or annulus (ring) with a vortex were found. Further, the creation of additional vortices by the FM near the surface was described,⁸ by a simple comparison of the free energies of the system with and without the vortex. However, the spontaneous creation of a vortex-antivortex pair as a possible lower energy state was never considered.

Other theoretical studies involving finite-size ferromagnets were mainly restricted to the problem of a magnetic dot with out-of-plane magnetization embedded in a supercon-

ducting film.^{10,11} Marmorkos *et al.*¹⁰ were the first to solve the nonlinear Ginzburg-Landau (GL) equation numerically, with appropriate boundary conditions for an infinitely long ferromagnetic cylinder penetrating the superconducting film, and found a correspondence between the value of the magnetization and the vorticity of the most energetically favorable giant-vortex state. The vortex structure of a SC disk with a smaller magnetic disk on top of it was numerically calculated in Ref. 12 using the first nonlinear GL equation, i.e., neglecting the effect of the screening currents on the total magnetic field. Interesting vortex-antivortex configurations and an interplay between the giant-vortex and multivortices were found.

Most recently, the pinning of vortices by small magnetic particles was studied experimentally¹³⁻¹⁵ which was a motivation for our recent theoretical study of this system.¹⁶ In the latter study we approximated the magnetic-field profile by a magnetic dipole. In the present paper, we generalize these results in order to include the *realistic magnetic-field profile* of the FM which in the present approach can be of arbitrary shape. The superconducting film lies in the xy plane while the FM is positioned a distance l above the SC, and is magnetized in the positive z direction (out of plane). To avoid the proximity effect and the exchange of electrons between the FM and the SC we assume a thin layer of insulating oxide between them as is usually the case in the experiment.

The paper is organized as follows. In the following section we present the general formalism. In Sec. III, we discuss the pinning potential of the magnetic disk and magnetic annulus (ring) with out-of-plane magnetization. Further, the vortex-magnet interaction energy and supercurrent induced in the superconductor are calculated analytically and the profiles are shown. We use these results in Sec. IV to investigate the manipulation of vortices in the case of a more complicated geometry of the magnet, i.e., magnetic disk with an off-center hole(s). In Sec. V the pinning properties of the magnet with square or triangular shape are analyzed and the most favorable trajectory of the vortex with respect to the magnet edge is determined. The influence of edges (corners) of the FM on the pinning is then discussed and our conclusions are given in Sec. VI.

II. THEORETICAL FORMALISM

We consider a ferromagnet of arbitrary shape with homogeneous out-of-plane magnetization \vec{M} , placed outside a type II SC film interacting with a single vortex in the SC. Within the London approximation, the Gibbs free energy of this system is given by¹⁷

$$F = \frac{1}{8\pi} \int dV [\vec{h}^2 + \lambda^2 (\text{rot}\vec{h})^2] - \int dV [\vec{h}_v \cdot \vec{M}], \quad (1)$$

where λ is the penetration depth, \vec{h} is the total field present in the system, and \vec{h}_v and \vec{M} denote the magnetic field of the vortex and magnetization of the FM, respectively. The second integral in Eq. (1) represents the potential energy of the FM in the magnetic field of the vortex. In this paper, we focus on the ferromagnet-vortex interaction energy, and the terms in Eq. (1) regarding the self-energy of the vortex and the magnet are omitted. In the case of a point magnetic dipole, the second integral in Eq. (1) corresponds to the exclusion of the volume of the FM when integration is performed (see Ref. 16 and references therein).

The direct interaction energy between the vortex and the FM in a stationary magnet-superconductor system is given by¹⁶

$$U_{mv} = \frac{1}{2c} \int dV^{(i)} [\vec{j}_m \cdot \vec{\Phi}_v] - \frac{1}{2} \int dV^{(fm)} \vec{h}_v \cdot \vec{M}, \quad (2)$$

where $\vec{\Phi}_v = (\Phi_\rho, \Phi_\varphi, \Phi_z) = (0, \Phi_0 / (2\pi |\vec{\rho} - \vec{\rho}_v|), 0)$ denotes the vortex magnetic flux vector in London approximation (Φ_0 is the flux quantum and $\vec{\rho}_v$ denotes the position of the vortex). The first integration is performed over the volume $V^{(i)}$ inside the superconductor, while $V^{(fm)}$ in the second integral denotes the volume of the ferromagnet. Indices v and m refer to the vortex and the magnet, respectively, \vec{j} denotes the current, and \vec{h} the magnetic field.

The interaction energy in this system consists of two parts: (i) the interaction between the Meissner currents generated in the SC (\vec{j}_m) by the FM and the vortex and (ii) the interaction between the vortex magnetic field and the FM. In the Appendix, we show analytically that in the case of a point magnetic dipole (MD) these two contributions are equal. Due to the superposition principle, the finite FM's with homogeneous magnetization can be represented as an infinite number of dipoles. Consequently, in our case of out-of-plane magnetized FM, the vortex-magnet interaction energy equals

$$U_{mv} = - \int dV^{(fm)} \vec{h}_v \cdot \vec{M}. \quad (3)$$

In order to obtain the current induced in the superconductor by the ferromagnet, one should solve first the equation for the vector potential¹⁵

$$\text{rot}(\text{rot}\vec{A}_m) + \frac{1}{\lambda^2} \Theta(d/2 - |z|) \vec{A}_m = 4\pi \text{rot}\vec{M}. \quad (4)$$

This equation is rather complicated to be handled for a finite-size FM, but the analytic expressions for the induced SC current in an infinite superconducting film with thickness d ($-d/2 < z < d/2$) in the MD case (with magnetic moment m) are known¹⁶ as

$$j_x^{md}(x, y, z) = \frac{cm\Phi_0}{2\pi\lambda^3} \frac{y_m - y}{R_m} \int_0^\infty dq \exp\left\{-q\left(|z_m| - \frac{d}{2}\right)\right\} \times q^2 J_1(qR_m) C(q, z), \quad (5a)$$

$$j_y^{md}(x, y, z) = \frac{cm\Phi_0}{2\pi\lambda^3} \frac{x - x_m}{R_m} \int_0^\infty dq \exp\left\{-q\left(|z_m| - \frac{d}{2}\right)\right\} \times q^2 J_1(qR_m) C(q, z), \quad (5b)$$

with

$$C(q, z) = \frac{k \cosh\left[k\left(\frac{d}{2} + z\right)\right] + q \sinh\left[k\left(\frac{d}{2} + z\right)\right]}{(k^2 + q^2) \sinh(kd) + 2kq \cosh(kd)}, \quad (6)$$

where $k = \sqrt{1 + q^2}$, $R_m = \sqrt{(x - x_m)^2 + (y - y_m)^2}$ is the distance between the dipole and the point of interest, and $J_\nu(\alpha)$ is the Bessel function. The coordinates (x_m, y_m, z_m) denote the position of the dipole. The magnetic moment of the magnet is measured in units of $m_0 = \Phi_0 \lambda$, and all distances are scaled in units of λ . These units will be used in the rest of the paper.

To find the supercurrent induced by a finite-size FM above the superconductor, we make use of the superposition principle and consequently the above expressions (5) and (6) have to be integrated over the volume of the ferromagnet. Thus, the value of the current is given by ($\alpha = x, y$)

$$j_\alpha(x, y, z) = \int j_\alpha^{md}(x, y, z) dV^{(fm)}. \quad (7)$$

III. MAGNETIC DISK (RING)-VORTEX INTERACTION

In this section, we investigate the interaction between a vortex in an infinite type II superconducting film with thickness d ($-d/2 < z < d/2$) and the magnetic disk with radius R and thickness D with *out-of-plane magnetization*, i.e., $\vec{M} = \Theta(R - \rho) \Theta(z_1 - z) \Theta(z - z_0) m \vec{e}_z / (R^2 \pi D)$ (in units of $M_0 = \Phi_0 / \lambda^2$) located at distance l above (under) the SC ($z_0 = l$, $z_1 = l + D$).

Inserting the well-known expression for the magnetic field of a vortex outside the SC [see Eqs. (A4) and (A5) in the Appendix] into Eq. (3) we find the following expression for the magnetic disk-vortex interaction:

$$U_{mv} = \frac{MR\Phi_0^2}{\lambda} U_\perp(\rho_v), \quad (8a)$$

where $\rho = \rho_v$ denotes the position of the vortex and

$$U_{\perp}(\rho_v) = \int_0^{\infty} dq \frac{1}{qQ} J_1(qR) J_0(q\rho_v) E(q, l, D), \quad (8b)$$

where

$$Q = k[k + q \coth(kd/2)]$$

and

$$E(q, l, D) = e^{-ql}(e^{-qD} - 1).$$

For the case of a thin ferromagnetic disk above the thin superconducting film ($d, D < 1$), the following asymptotics can be obtained:

(1) for $\rho_v < R$, we found

$$U_{\perp}(\rho_v) \approx -\frac{dDR}{2} \left(\frac{1}{l + \sqrt{l^2 + R^2}} - \frac{\rho_v^2}{4} \frac{1}{(l^2 + R^2)^{3/2}} \right); \quad (9a)$$

(2) for $\rho_v > R$ and $\rho_v \sim l$,

$$U_{\perp}(\rho_v) \approx -\frac{dDR}{4} \left(\frac{1}{\sqrt{l^2 + \rho_v^2}} - \frac{R^2}{8} \frac{2l^2 - \rho_v^2}{(l^2 + \rho_v^2)^{5/2}} \right); \quad (9b)$$

(3) for $\rho_v > R, l$,

$$U_{\perp}(\rho_v) \approx -\frac{dDR}{4} \left(\frac{1}{\sqrt{l^2 + \rho_v^2}} - \frac{d\pi}{4} \left[H_0\left(\frac{\rho_v d}{2}\right) - Y_0\left(\frac{\rho_v d}{2}\right) \right] \right). \quad (9c)$$

Here, $H_v(x)$ and $Y_v(x)$ denote the Struve and Bessel functions, respectively.

In the case of a FM on top of the SC ($l=0$), the above asymptotics [9(a)–(c)] can be expressed in a more precise way:

(1) for $\rho_v < R$,

$$U_{\perp}(\rho_v) \approx -\frac{dD}{\pi} E\left(\frac{\rho_v^2}{R^2}\right); \quad (10a)$$

(2) for $\rho_v > R$,

$$U_{\perp}(\rho_v) \approx -\frac{dDR}{\pi} \left\{ \frac{1}{\rho_v} \left[\frac{\rho_v^2}{R^2} E\left(\frac{R^2}{\rho_v^2}\right) + \left(1 - \frac{\rho_v^2}{R^2}\right) K\left(\frac{R^2}{\rho_v^2}\right) \right] + \frac{d\pi^2}{16} \left[H_0\left(\frac{\rho_v d}{2}\right) - Y_0\left(\frac{\rho_v d}{2}\right) \right] \right\}. \quad (10b)$$

$K(x)$ and $E(x)$ are the complete elliptic integrals of the first and second kind, respectively. Further expansion of the asymptotic behavior of the energy at large distances [Eqs. (9c) and (10b)] gives $U_{\perp}(\rho_v) \approx -DR/d\rho_v^3$.

When we take the derivative of the interaction energy, Eq. (8), over ρ_v we obtain the force acting on a vortex in the presence of a magnetic disk:

$$F_{mv} = \frac{MR\Phi_0^2}{\lambda^2} F_{\perp}(\rho_v), \quad (11a)$$

with

$$F_{\perp}(\rho_v) = \int_0^{\infty} dq \frac{1}{Q} J_1(qR) J_1(q\rho_v) E(q, l, D). \quad (11b)$$

For the case of a thin FM on top of a thin SC ($d, D < 1, l=0$), we derived the following asymptotics:

(1) for $\rho_v < R$,

$$F_{\perp}(\rho_v) \approx \frac{dD}{\pi\rho_v} \left[E\left(\frac{\rho_v^2}{R^2}\right) - K\left(\frac{\rho_v^2}{R^2}\right) \right]; \quad (12a)$$

(2) for $\rho_v > R$,

$$F_{\perp}(\rho_v) \approx \frac{dD}{\pi R} \left[E\left(\frac{R^2}{\rho_v^2}\right) - K\left(\frac{R^2}{\rho_v^2}\right) \right] - \frac{d^3DR}{16} \frac{\pi}{2} \left[Y_1\left(\frac{\rho_v d}{2}\right) + H_{-1}\left(\frac{\rho_v d}{2}\right) \right]. \quad (12b)$$

The latter expression reduces in the extreme $\rho_v \gg R$ limit to $F_{\perp}(\rho_v) \approx -3DR/d\rho_v^4$, which is consistent with the asymptotic behavior of the interaction energy.

The results for the full numerical calculation of Eq. (8) are shown in Fig. 1(a) for a magnetic disk with radius $R=3.0$, and three values of the thickness $D=0.1, 0.5, 1.0$, fixed total magnetic moment $m=1.0$ ($M=m/V^{(fm)}$), and at distance $l=0.1$ above the SC with thickness $d=0.1$. The energy is expressed in units of $U_0 = \Phi_0^2/\pi\lambda$ and the force in $F_0 = \Phi_0^2/\pi\lambda^2$. The magnetic-vortex interaction increases if the magnet is made thinner, since the magnetization in that case increases due to the fact that the magnetic moment of the magnetic disk is kept constant in this calculation. Also the magnetic field of the disk becomes more peaked near the magnet edge. In Fig. 1(b), the dependence of the interaction energy on the thickness of the SC is shown. The increased thickness of the SC makes the interaction stronger, due to the stronger response of the SC to the presence of the magnet. Note that increasing the thickness beyond $d \gg \lambda$ does not influence the energy [dashed curve in Fig. 1(b), $Q \approx k(k+q)$ in Eq. (8)]. The vortex is attracted by the magnetic disk when the magnetization and the vortex are oriented parallel, independently of the value of the parameters. The interaction energy has its minimum just under the center of the disk, which is the energetically most favorable position of the vortex. The force acting on the vortex is purely attractive and it has its maximum at the edge of the magnetic disk [see Fig. 1(c)]. For large distances between the magnetic disk and the vortex the interaction approaches the value obtained earlier for the case of a magnetic dipole.¹⁶ Note that in the limit $R \rightarrow 0$ and $D \rightarrow 0$, Eq. (8) corresponds to the out-of-plane dipole case of Ref. 16. In Refs. 8 and 9 the interaction energy

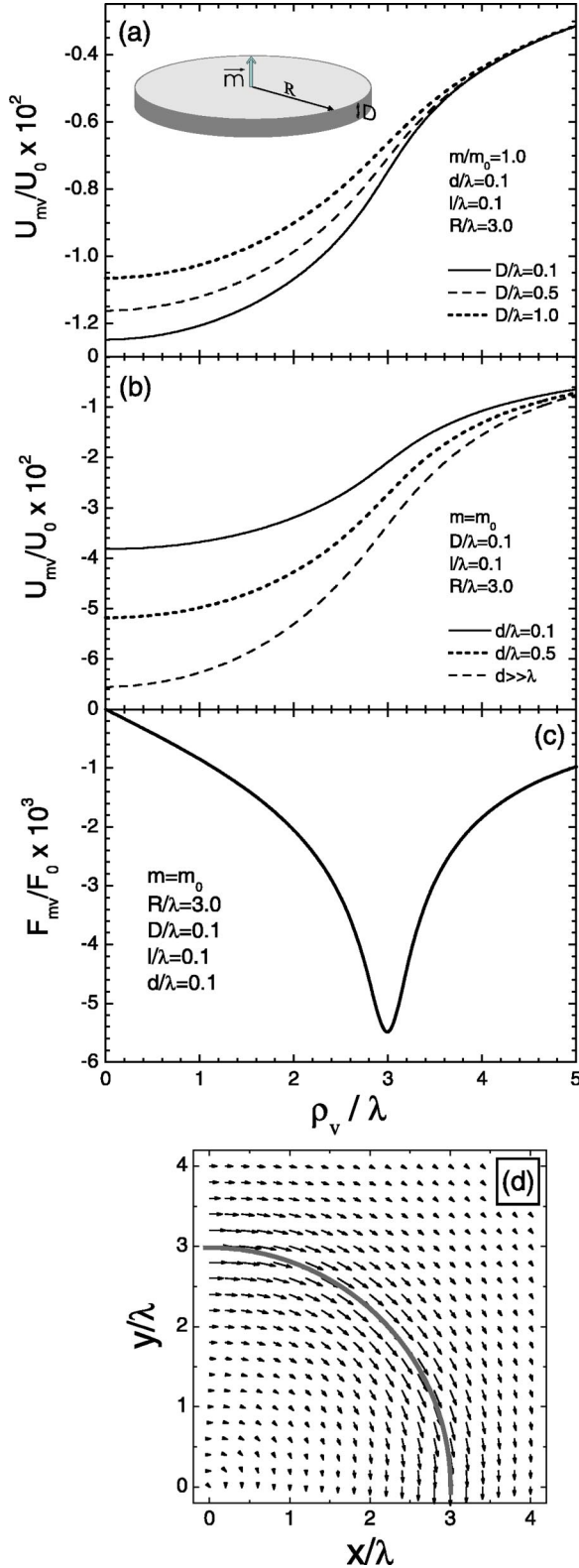


FIG. 1. The magnetic disk-vortex interaction energy as a function of the distance between the vortex and the center of the FM disk: for several values of (a) the thickness of the FM disk and (b) the thickness of the SC. (c) Plot of the FM-vortex force and (d) a vectorplot of the current induced in the SC due to the presence of the FM [same parameters as in (c)]. The gray semicircle in (d) indicates the position of the edge of the FM.

between a magnetic nanostructure and a vortex in a thin superconductor ($d \ll \lambda$) was calculated. In that case, the thickness of the magnet was not taken into account (assumed to be infinitely thin), the superconducting film was taken very thin ($d \ll \lambda$), and the FM was placed on top of the SC (in the same $z=0$ plane) which corresponds to $l=0$ in our case. In these limits, our equations reduce to the same expressions for the interaction energy like those given in Refs. 8 and 9. But note that the analytical expressions are still not completely reached in the distance range shown in Fig. 1 and therefore a numerical calculation of the full integral is necessary in order to obtain the magnet-vortex interaction energy. Therefore, from this point of view, our expression offers much more information (nonzero thickness of both FM and SC, and arbitrary position of the FM above the SC) without a real increase of the complexity of the numerical calculation.

To better understand the attractive magnet-vortex behavior in this system, we calculated the supercurrent induced in the SC due to the presence of the magnet. As explained in Sec. II, this current can be obtained after integration of Eq. (7). In the case of a flat magnetic disk, it has only an azimuthal component and reads

$$j_\varphi(\rho, z) = \frac{cMR\Phi_0}{\lambda^3} \int_0^\infty dq J_1(qR) J_1(q\rho) E(q, l, D) C(q, z), \quad (13)$$

where $\rho = \sqrt{x^2 + y^2}$ and $C(q, z)$ is given by Eq. (6). For a FM placed under the SC, one should replace z by $-z$. The vectorplot of the current is shown in Fig. 1(d). One should notice that the direction of the current is the one normally associated with an antivortex (the clockwise direction) and that the current is maximal at the magnetic disk edge. This agrees with our previous results: the direction of the current explains the attraction between the FM disk and the vortex, and the position of the maximum of the current corresponds to the maximal attractive force. The problem is cylindrically symmetric, and a vortex approaching the magnet from any direction will be attracted for parallel alignment and repelled in the antiparallel case. This important point was not fully explained in Ref. 9.

Using the same procedure, for a magnetic annulus ($R_i < \rho < R_o$) with thickness D and out-of-plane magnetization [inset of Fig. 2(b)] we have

$$\vec{M} = \frac{1}{V_{ann}} \Theta(\rho - R_i) \Theta(R_o - \rho) \Theta(z_1 - z) \Theta(z - z_0) m \vec{e}_z, \quad (14)$$

resulting in the vortex-magnet interaction energy

$$U_{mv} = \frac{M\Phi_0^2}{\lambda} \int_0^\infty dq \frac{1}{qQ} J_0(q\rho_v) \times [R_o J_1(qR_o) - R_i J_1(qR_i)] E(q, l, D). \quad (15)$$

The interaction energy and force curves for the magnetic annulus-vortex interaction are given in Figs. 2(a,b) and are in

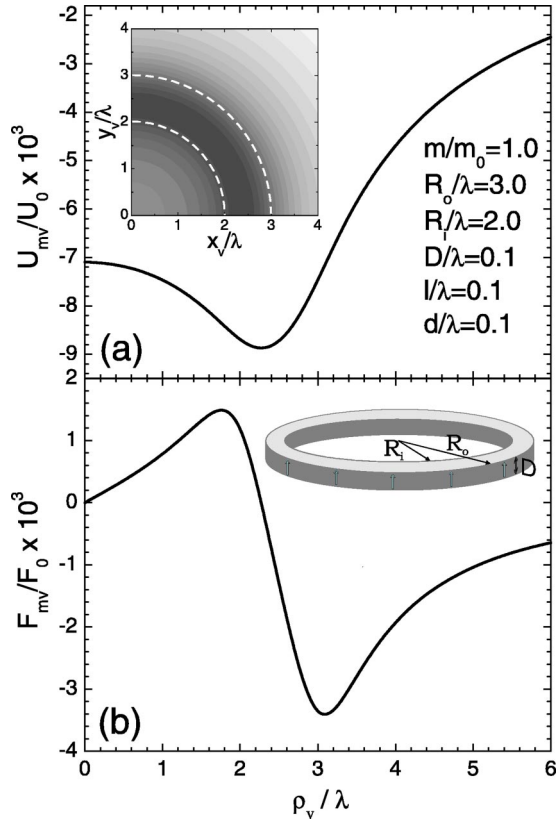


FIG. 2. The out-of-plane magnetized annulus-vortex interaction: (a) the interaction energy and (b) plot of the FM-vortex force. The contourplot of the interaction energy is shown as inset in (a) (dark color illustrates low energy, as will be the case throughout the paper, the dashed white semicircles illustrate the edges of the magnet). A schematic outline of the magnetic annulus is shown in the inset of (b).

qualitative (but not quantitative) agreement with the earlier results of Ref. 7, which were obtained in the limit of an extremely thin SC and FM, namely, $d, D \ll \lambda$. Please notice again that in our calculation finite thicknesses of both SC and FM are fully taken into account. The most important result is that, in this case, the annulus-vortex interaction energy has a ringlike minimum, under the magnet. The exact radial position of this minimum depends on the SC parameters, the thickness of the magnet, and its distance from the SC. The force acting on the vortex shows dual behavior—attractive outside the equilibrium ring and repulsive inside.

Due to the dual behavior of the FM-vortex force one naively expects different current flow in the superconductor inside and outside the annulus. We use again Eq. (7) and for the current induced in the superconductor we obtain

$$j_\varphi(\rho, z) = \frac{cM\Phi_0}{\lambda^3} \int_0^\infty dq [R_o J_1(qR_o) - R_i J_1(qR_i)] \times J_1(q\rho) E(q, l, D) C(q, z). \quad (16)$$

In Fig. 3 we show a comparison between the currents induced in the SC in the case of a magnetic disk (dashed curves) and a magnetic annulus (solid curves), for different

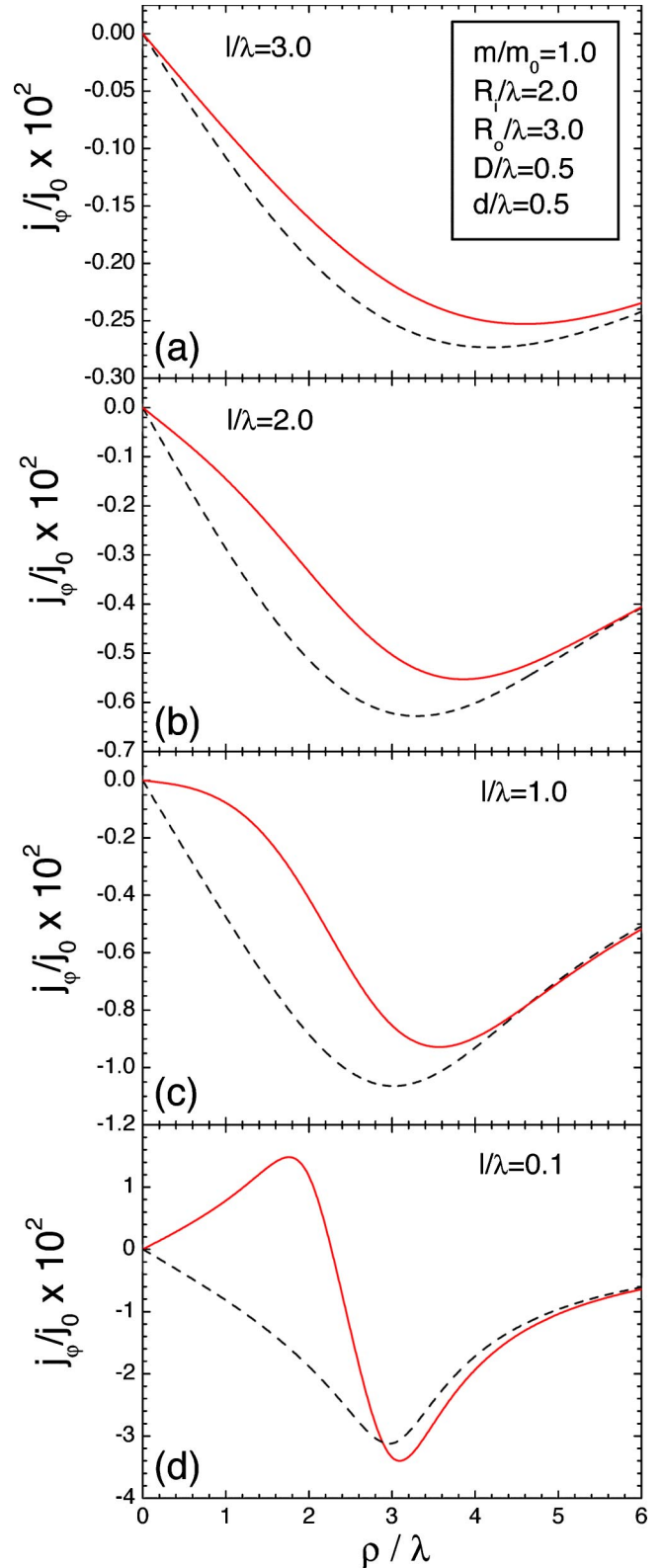


FIG. 3. Comparison between the currents induced in a SC (in units of $j_0=c\Phi_0/\lambda^3$) by a magnetic disk (dashed curves) and a magnetic annulus (solid curves) with the same outer radius, as the FM-SC vertical distance l decreases (a)–(d).

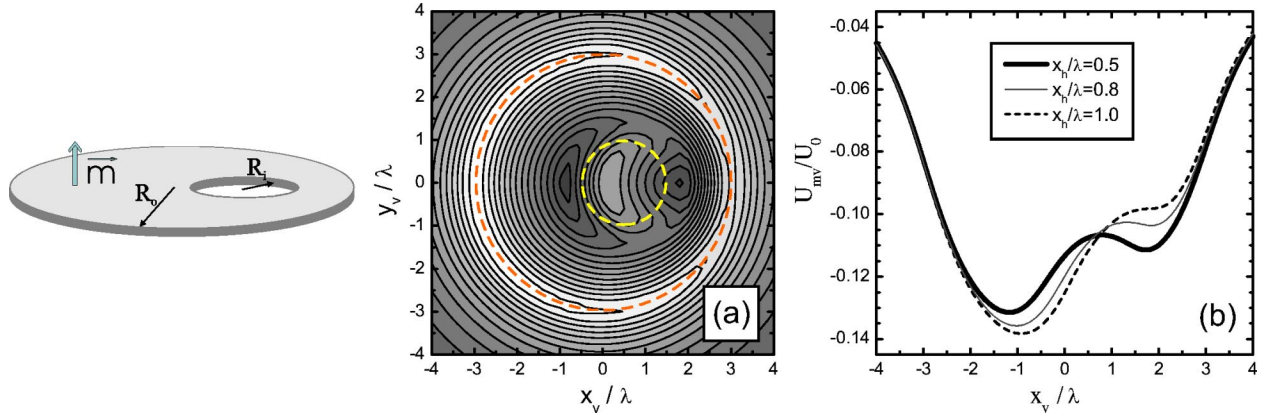


FIG. 4. The interaction of the vortex with a magnetic disk with an off-center hole (see left figure for schematics of the magnet configuration): (a) contourplot of the interaction energy for $R_o=3.0$, $R_i=1.0$, $(x_h, y_h)=(0.5, 0)$, $l=0.1$ and $D=d=0.5$, with $M=M_0$ (dashed circles indicate the edges of the magnet), and (b) the energy along the x axis, for three different locations of the off-center hole in the magnetic disk.

SC-FM vertical distances. When the magnet is positioned far above the superconductor, the vortex qualitatively does not feel the difference between the disk and the ring case, and the current induced in the SC shows a similar behavior [Fig. 3(a)]. When approaching the superconductor, the influence of the central hole in the ring becomes more pronounced [Figs. 3(b,c)], and eventually the current changes sign [Fig. 3(d)].

Obviously, the qualitative behaviors of all quantities outside the annulus approach those for the case of a magnetic disk. However, inside the ring, the situation is different. The nature of the magnet-vortex force changes and while the current flows in the clockwise direction outside the ring, inside the superconductor the direction of the current is anticlockwise in the case of a small FM-SC distance [i.e., $l/\lambda=0.1$, Fig. 3(d)]. Please notice that due to the fact that the finite thickness of the SC is included in our calculations, the SC current contains also a z dependence [i.e., through the $C(q, z)$ function].

From a look at Eqs. (15) and (16), one can see that the problem of a magnetic annulus actually can be modeled by two concentric magnetic disks with different radii and opposite magnetization. The problem is linear, and this will facilitate the calculation in the cases of noncylindrically symmetric FM's.

IV. MANIPULATION OF THE EQUILIBRIUM VORTEX POSITION WITH A MAGNETIC DISK CONTAINING A CAVITY

In the preceding section, we discussed the pinning of vortices by a magnetic disk or annulus (ring). We showed that the most energetically favorable position for the vortex is under the center of the magnetic disk (for parallel alignment) or under the annulus (equilibrium ring). Here we generalize the latter system and displace the hole in the disk from its central location.

Referring to the preceding section, we may consider this problem as a superposition of effects of two magnetic disks with opposite magnetization. The smaller radius magnetic disk with the opposite magnetization models the hole in the

larger disk. The parameters of the magnet are the outer radius R_o , the radius of the hole R_i , the center of the hole is at (x_h, y_h) , and the thickness of the FM is denoted by D . Therefore, using Eqs. (8)–(13) for two magnetic disks, one with radius R_o and the other with radius R_i , with opposite magnetization and centered at $(x, y)=(0, 0)$ and (x_h, y_h) , respectively, we investigate the pinning properties of such a FM.

The results of this calculation are shown in Fig. 4 for a magnetic disk with $R_o=3.0$, $R_i=1.0$, $(x_h, y_h)=(0.5, 0)$, $l=0.1$, and $D=d=0.5$. In Fig. 4(a) we show the contourplot of the FM-vortex attractive force. It is clear that there are two local energy minima along the $y=0$ direction, where the force equals zero: in front of and behind the hole. In Fig. 4(b) the plot of the interaction energy is given along this direction for three positions of the hole $x_h=0.5, 0.8$, and 1.0 . The important result is that the two minima are not equal: the one closer to the outer edge of the magnet has higher energy (metastable state) and the one near the magnet center is the actual ground state. However, due to the presence of the hole, the equilibrium position of a vortex is not exactly in the center, and depends on the position of the hole. The magnet is not cylindrically symmetric and we have two separate energy minima instead of a ring of minima as in the case of the magnetic annulus. Also, one could argue that a slowly moving vortex in a system with no temperature fluctuations could be trapped at the metastable position. Anyhow, the hole in a magnetic disk appears to be a powerful tool for a possible manipulation of the vortex position. However, one question arises: since there are two minima present in the interaction energy, is it possible to have two equilibrium states with the same energy?

In order to construct such a situation, we introduced a second hole in the magnet, at a symmetrical position to the first one with respect to the center of the magnet. As an example, we took the parameters of the magnet as $R_o=3.0$, R_i (for both holes) $=0.5$, and $(x_h, y_h)=(\pm 1.0, 0)$. The interaction energy along the x axis is given in Fig. 5. Two equal minima near the outer edge of the disk are

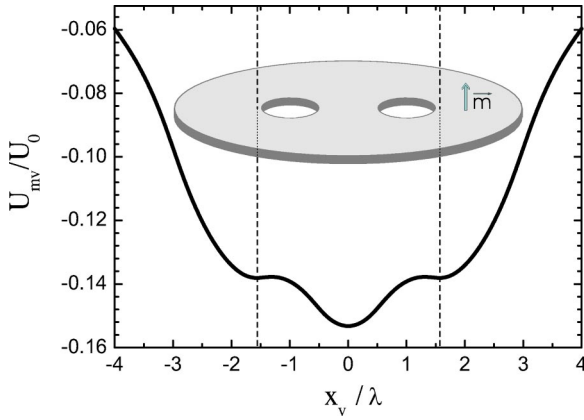


FIG. 5. The magnetic disk with two symmetrical holes: plot of the FM-vortex interaction energy illustrating the position of the metastable and ground vortex states with respect to the position of the holes (dashed vertical lines). The parameters of the system are $R_o=3.0$, R_i (for both holes) $=0.5$, $(x_h, y_h)=(\pm 1.0, 0)$, $l=0.1$, $D=d=0.5$, and $M=M_0$.

found next to the magnet holes. However, the global minimum is still under the center of the magnet (see inset of Fig. 5). To eliminate this minimum we allow the holes to touch each other and to form an “eight-hole” in the center of the magnet. The resulting interaction energy [Fig. 6(a)] has now only two equal minima along the $y=0$ direction, outside the hole, near the magnet edge, and a plateaulike behavior in the central region. Still, these minima are not the lowest energy states. The central global minimum of the interaction energy from the previous case is now split by the joined holes into two minima along the $x=0$ direction [see Fig. 6(b)]. The latter minima represent the ground state for a vortex in the presence of a magnetic disk with an eight-hole. The vortex has two absolutely equal ground states and the same probability of eventually sitting in one of those. Thanks to this feature, a possible use of this system for quantum computing can be analyzed, similar to the quantum systems proposed before (see, for example, Ref. 18).

In Fig. 6(c) the contourplot of the magnet-vortex interaction energy is given, together with a vectorplot of the current induced in the SC. The position of the eight-hole is denoted by the thick solid circles. Around the magnetic disk, the SC current flows in a clockwise direction, illustrating the general attraction between the FM and the vortex. However, under the magnet, current shows a dual behavior, and a vortex-antivortexlike current flow can be seen. Namely, at the equilibrium vortex-states we find “antivortex” current profiles while under the holes of the magnet a vortexlike current motion is present. This suggests the possibility that such a magnetic-field configuration, for sufficiently strong magnetization, could induce interesting vortex-antivortex configurations if placed near a superconducting film.

Using this approach, interaction of a vortex with magnets of more complicated shapes can be investigated. We have shown that the magnetic disk with a cavity is a nice example of how to control the vortex by the magnet geometry. From the point of view of practical vortex manipulation, it would

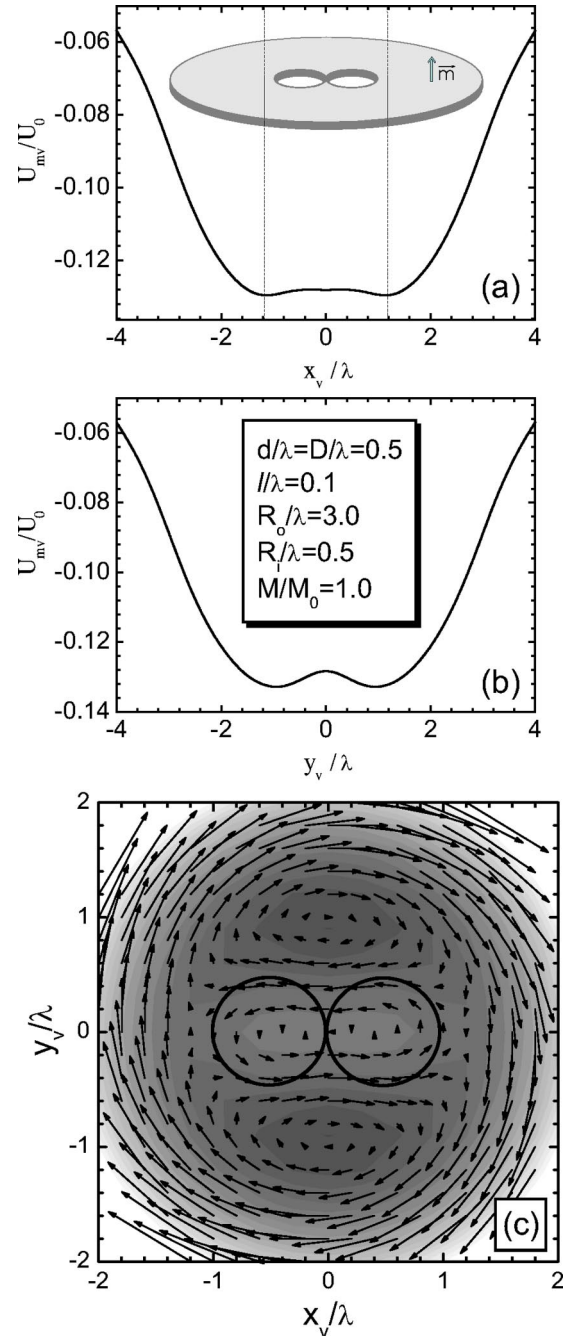


FIG. 6. The interaction energy of a vortex with a magnetic disk containing an “eight-hole”: (a) interaction energy for the vortex positioned along the x axis at the $y=0$ line, (b) along the y axis for $x=0$, and (c) contourplot of the FM-vortex interaction energy (dark color–low energy). In (c) the vectorplot of the current induced in the SC in the presence of the FM is superimposed. The solid circles denote the position of the holes in the FM above the SC.

be interesting to move the vortex by changing the parameters of the system. Helseth⁹ proposed a system in which a magnetic disk (with magnetization M_1) is placed in the center of a magnetic ring (with magnetization M_2), where the disk and the ring can have opposite magnetization. In Fig. 7 we show the outline of the system (upper inset), and the calculated interaction energy and force acting on the vortex, for

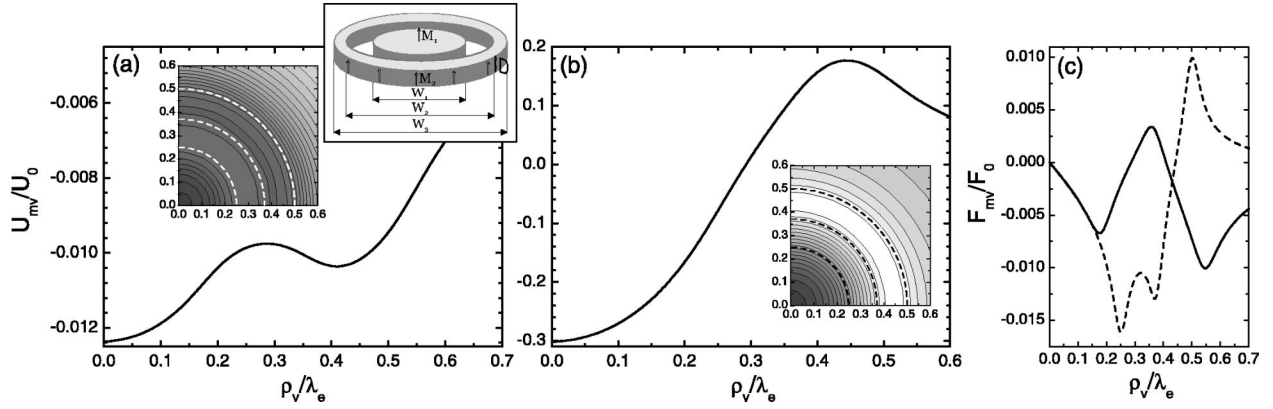


FIG. 7. Disk-ring magnetic structure [see inset of (a) for a schematic view of the configuration] above the SC: (a) FM-vortex interaction energy for $M_1=M_2$ and (b) for $M_2=-M_1$. The contourplots of the energy are given as insets (dashed lines indicate the edges of the magnet). The force acting on the vortex is shown in (c), as the solid curve for case (a) and dashed one for case (b). The parameters are $W_1=0.5$, $W_2=0.75$, $W_3=1.0$, $D=0.01$, and $l=0.001$, all in units of the effective penetration depth $\lambda_e=\lambda^2/d$.

the parameters $W_1=0.5\lambda_e$, $W_2=0.75\lambda_e$, $W_3=1.0\lambda_e$, and $D=0.1\lambda$ on top of a SC with thickness $d=0.1\lambda$. Here $\lambda_e=\lambda^2/d$ denotes the effective penetration depth. We suppose a thin oxide layer between the SC and the FM with thickness 0.01λ . First we consider the $M_1=M_2$ case. Helseth claimed that in this case, a slowly moving vortex will be attracted and sit under the annulus. The plot of the interaction energy in Fig. 7(a) shows two energy minima, namely, under the disk, and under the annulus [(ring-energy minimum, see inset of Fig. 7(a))].

From our calculations it is clear that the ground state for the vortex would be in the center of the magnetic vortex, while a metastable state exists under the annulus as claimed in Ref. 9. However, one could argue that a vortex, slowly moving towards the magnet, could rest in a metastable state under the ring, if there are no fluctuations in the system. In Fig. 7(c), the solid line shows the force acting on the vortex. Please note that in our calculation, the positions of the extremes correspond to the magnet edges, while in Ref. 9 this was not the case. Also, the peaks in the forces in our calculation are much smaller, due to the finite thickness of the magnet. It should be noted that the relation between the two energy minima and the acting forces strongly depends on the parameters and it can change in favor of the annulus if it is made wider.

In Ref. 9 it is also stated that in the opposite case, when the annulus magnetization changes sign, i.e. $M_2=-M_1$, the vortex is attracted to the center of the disk. The interaction energy we calculated in this case is plotted in Fig. 7(b) [the force is given in Fig. 7(c) by the dashed line]. It is clear that the annulus forms an energetic barrier which prevents a “slowly moving” vortex from reaching the central position. However, the global minimum of the energy is under the center of this magnetic structure [the energy shown in Fig. 7(b) decreases monotonously and reaches zero at infinity], implying that the vortex would definitely sit under the magnet for the considered parameters. Different values for R_1 , R_2 , R_3 could make the central minimum higher, and the energy barrier would then be able to repel the vortex. To

conclude, in order to use this magnetic structure for vortex manipulation, one should not only overcome the experimental difficulties to realize such a structure but also be careful about the influence of the parameters on the behavior of this system.

V. SQUARE AND TRIANGULAR MAGNETIC DISKS: INFLUENCE OF THE CORNERS ON THE VORTEX PINNING

Up to this point, we have only considered the interaction of a vortex with magnets having circular symmetry, namely magnetic disks, rings, and combinations of those. Here we consider FM's with broken circular symmetry, namely, square or triangular magnetic disks. We put the center of our Cartesian coordinates in the center of the magnet and the x axis along one of its sides. In this case, Eq. (3) cannot be solved analytically, and triple numerical integrations must be performed. In the case of a rectangular FM we have

$$U_{mv}(x_v, y_v) = \frac{M\Phi_0^2}{2\pi\lambda} \int_0^\infty \frac{dq}{Q} E(q, l, D) \times \int_{-A/2}^{A/2} dx \int_{-B/2}^{B/2} dy J_0(qR_v), \quad (17)$$

where $R_v = \sqrt{(x-x_v)^2 + (y-y_v)^2}$. A and B are the dimensions of the magnet (with thickness D) in the x and y directions, respectively. As before, the distance between the FM and the SC surface is l .

The components of the current induced in the SC are obtained in an analogous way, by numerical integration of Eq. (7), using the expressions (5a)–(6). In Fig. 8(a) the interaction energy with a vortex is shown, along two directions (lines of symmetry) (i) diagonal (dotted line); (ii) horizontal (solid line). In the inset, the contourplot of the energy is given. For comparison, we also give the results for a mag-

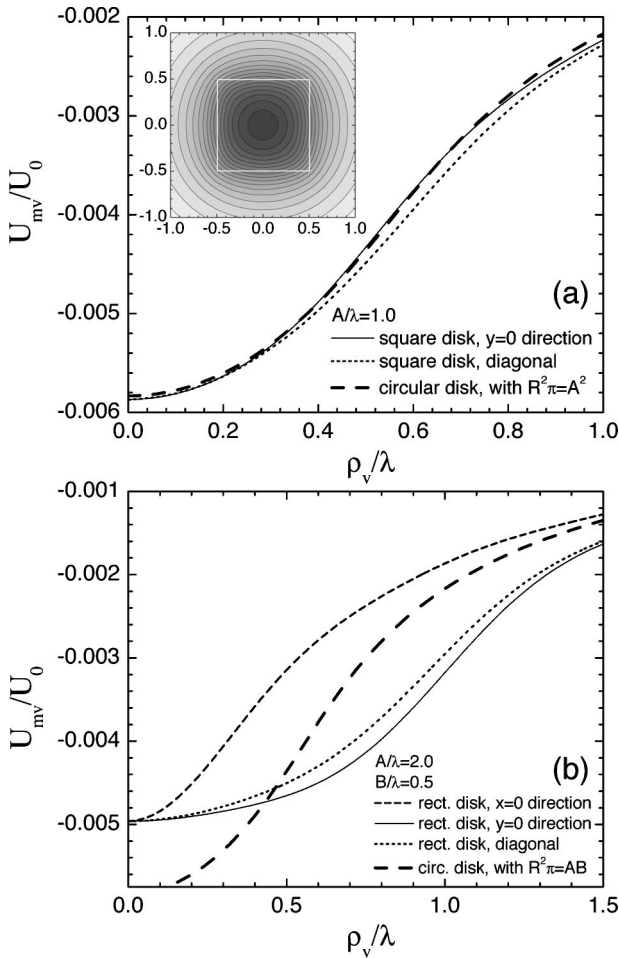


FIG. 8. Rectangular magnetic disk above a SC film: (a) FM-vortex interaction energy for a square magnet case, namely, with sides $A=B=1.0\lambda$, thickness $D=0.1\lambda$, and magnetization $M=M_0$, at $l=0.1$ above the SC with thickness $d=0.1\lambda$ (the inset shows the contourplot of the energy, white line indicates the edge of the magnet), and (b) for $A=4B=2.0$. For comparison, the FM-vortex interaction energy in the case of the magnetic disk with the same volume is given by the thick dashed curves.

netic disk (thick dashed curve) with $R^2\pi=AB$ and the same thickness D . As far as the pinning potential of square magnetic disk is concerned, the asymmetry is rather small and the result is not much different from the one of an equivalent circular disk. Only in the region near the edge of the magnet, some discrepancy between the pinning potential of the square magnet in the diagonal direction and the disk approximation is observed. Moving further from the magnet, this discrepancy disappears. The energetically favorable position of the vortex is under the center of the magnet. The situation is somewhat different for rectangular-shaped FM disks. In Fig. 8(b) we show the results for $A=4B=2.0$ and, in this case, the corresponding circular disk becomes a very poor approximation. Far away from the magnet, this approximation becomes better, as expected. From the behavior of the interaction energy we have seen that the vortex is attracted to the center of the square or triangular magnet for parallel orientation of the magnetization and the vortex magnetic

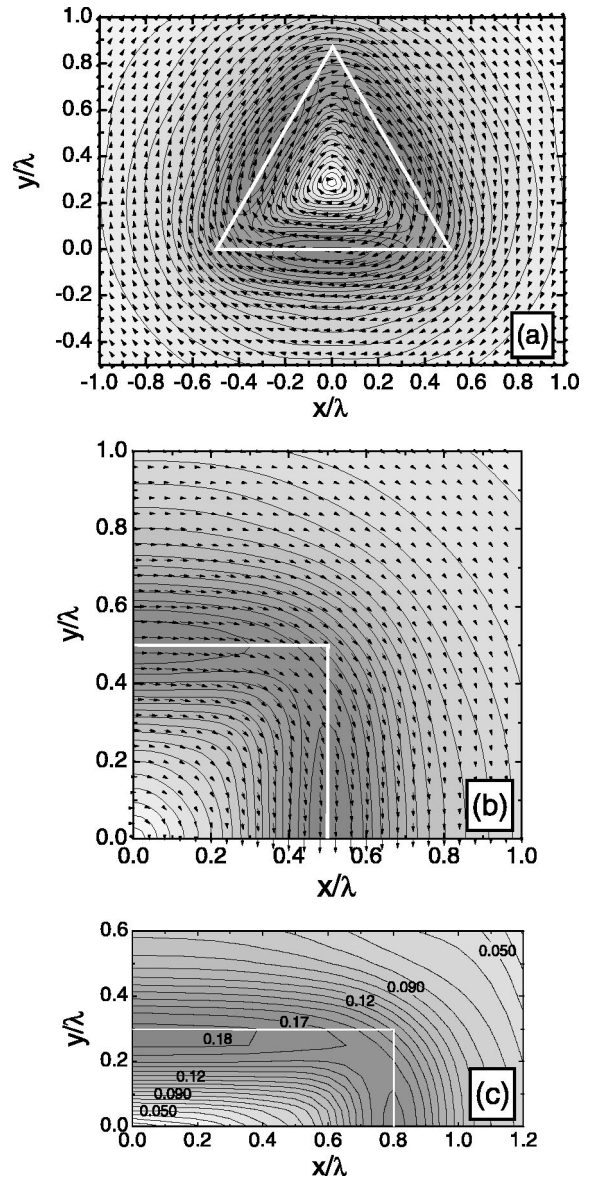


FIG. 9. The contourplots of the FM-vortex attractive force for parallel orientation of the magnetization and the vortex magnetic field, for (a) an equilateral triangular magnetic disk, with sides $a=1.0\lambda$ and (b) square magnet, with sides $A=B=1.0\lambda$. The other parameters correspond to the ones in Fig. 8. The vectorplots of the current are superimposed. In (c), the contourplot of the force for the rectangular magnet case is given, $A=1.6\lambda$, $B=0.6\lambda$. Dark color represents high force intensity. Positions of the edges of the magnets are given by white solid lines.

field. This corresponds qualitatively to the case of a magnetic disk. However, the broken circular symmetry of the magnet introduces some changes in the magnet-vortex interaction. In Fig. 9 we show the contourplot of the force acting on the vortex and the vectorplot of the current induced in the SC, both for the case of a square and triangular magnetic disks. It is obvious that the attractive force is stronger at the sides than at the corners of the magnet. Therefore, the vortex approaching the magnet at the side of the magnet will be attracted stronger than on the diagonal direction. As far as the

current is concerned, it has the direction associated with an antivortex. Near the magnet, the current follows the shape of the magnet and is maximal along the sides of the magnet. Further from the square or triangular magnet, the behavior of the current is more similar to the case of the circular magnetic disk. In Fig. 9(c) the rectangular magnet case is shown. One important feature should be noticed: the FM-vortex attraction force is stronger at the longer side of the rectangle.

As one can see in Fig. 9, the maxima of the FM-vortex interaction force are located on the sides of the magnet. Therefore, one may expect that the energetically preferable direction of vortex motion when attracted by the FM is perpendicular to its sides. To investigate this, we put the vortex in different positions [open dots in Fig. 10(a)] and follow its trajectory using molecular-dynamics simulations. In our quasistatistical case, if the vortex moves, the FM-vortex interaction force is opposed by viscous forces of the form $-\eta v_v$, where η is the viscosity coefficient and v_v the velocity of the vortex. In equilibrium, these forces are equal and the motion of the vortex can be analyzed. Since we were not interested in real-time simulations, we assumed $\eta=1$. The results are shown in Fig. 10(a). If the initial position of the vortex is along the lines of symmetry of the magnet, the vortex moves straight towards the center of the magnet. Otherwise, the trajectory of the vortex is distorted towards the corner of the magnet. It actually appears that the vortex avoids the maxima of the attractive force. This is counterintuitive but can be explained by the profile of the FM-vortex interaction energy, given in Figs. 10(b,c). One should notice the “wave” shape of the energy [if going along the ring around the magnet, see Fig. 10(b)]. Following a circle around the magnet, the energy has its minima at the corners of the magnet [denoted by black triangles in Figs. 10(b,c)] and the saddle points are on the sides (white triangles). The periodicity in Fig. 10(c) corresponds to the number of corners of the ferromagnetic disk. From Fig. 10 it is obvious that the interaction energy for any position of the vortex lowers steep not only towards the center of the magnet but also towards the corners. This induces the distortion of the vortex trajectory and gives the impression that the vortex approaching the magnet from the corners is more energetically favorable.

VI. CONCLUSION

We applied the London theory to investigate flux pinning in SC films due to the presence of a ferromagnet situated above (or under) the SC, where the finite thicknesses of both FM and the SC were fully taken into account. In the case of a magnetic disk or annulus (ring), we obtained analytic expressions for the FM-vortex interaction energy, force and the screening currents. We also derived the asymptotic behavior of the interaction potential and the force for specific values of the involved parameters. In the case of a magnetic disk with an off-center hole we showed the existence of two local minima in the FM-vortex interaction energy—the ground state and the metastable one. By changing the position of the hole, the position of the equilibrium moves with respect to the magnetic disk center. We also showed that in the case of a FM disk with two touching holes (eight-hole) two minima

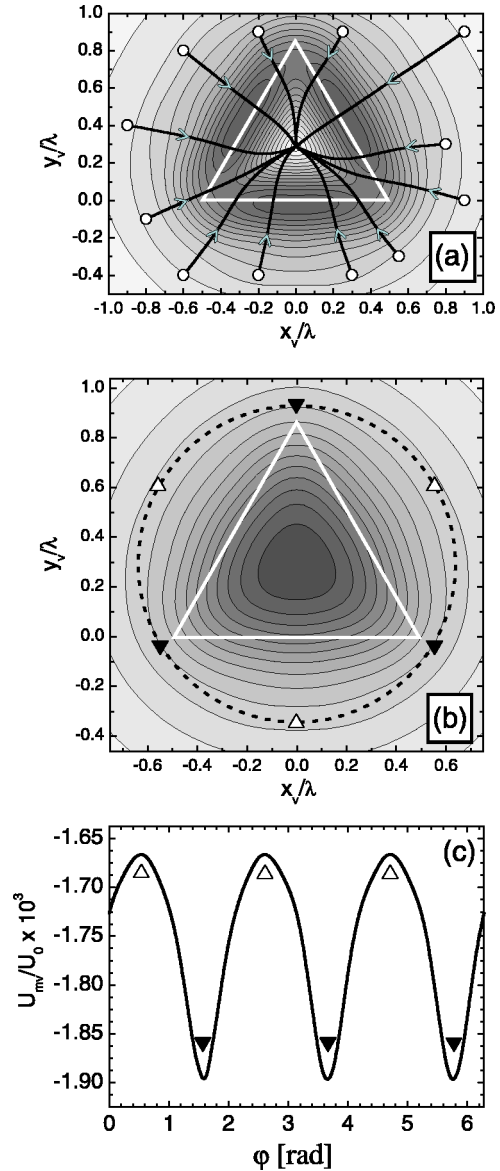


FIG. 10. The trajectory of the vortex when attracted by the triangular magnetic disk [same parameters as in Fig. 9(a)]: (a) vortex paths with respect to the attractive force landscape (the edge of the magnet is illustrated by white line), (b) the contourplot of the triangular magnet-vortex interaction energy (dark color—low energy), and (c) the interaction energy along the ring indicated by dashed line in (b).

with equal energy but different vortex positions appeared. The probability of a vortex sitting in one of these two states is the same, which makes this system interesting as a possible qubit. To further investigate the influence of the magnet geometry on its pinning properties, we calculated the pinning potential for square- and triangular-shaped ferromagnets. A substantial breaking of the circular symmetry occurs and the attractive force acting on the vortex is stronger at the sides of the magnet than at the corners. Also, making one side of the rectangular magnet longer enlarges the attractive force along it with respect to the other side. Although counterintuitive, we showed that the vortex approaches the noncircular mag-

net rather along the corners than perpendicular to the sides, following the gradient of the potential.

ACKNOWLEDGMENTS

This work was supported by the Flemish Science Foundation (FWO-VI), the Belgian Inter-University Attraction Poles (IUAP), the ‘‘Onderzoeksraad van de Universiteit Antwerpen’’ (GOA), and the ESF program on ‘‘Vortex matter.’’ Stimulating discussions with D. Vodolazov, V. V. Moshchalkov, and M. J. Van Bael are gratefully acknowledged.

APPENDIX: CALCULATION OF THE TWO CONTRIBUTIONS TO THE MAGNETIC DIPOLE-VORTEX INTERACTION ENERGY

The magnetic dipole-vortex interaction energy is given by¹⁶

$$F_{mv} = \frac{1}{2c} \int dV^{(i)} \vec{j}_m \cdot \vec{\Phi}_v - \frac{1}{2} \int dV^{(md)} \vec{h}_v \cdot \vec{M} = I_1 + I_2, \quad (\text{A1})$$

where $\vec{\Phi}_v = (\Phi_\rho, \Phi_\phi, \Phi_z) = (0, \Phi_0/(2\pi\rho), 0)$ denotes the vortex magnetic flux vector (Φ_0 is the flux quantum) and \vec{M} is the magnetization of the dipole. As one can see, the interaction energy in this system consists of two parts, namely, (i) the interaction between the Meissner currents generated in the SC (\vec{j}_m) by the MD and the vortex and (ii) the interaction between the vortex magnetic field and the MD. We will now separately calculate these contributions. The superconducting current induced in an infinite superconducting film with thickness d ($-d/2 < z < d/2$) by a magnetic dipole with *out-of-plane magnetization*, i.e., $\vec{m} = m\vec{e}_z$ located at $z = a$ ($l = a - d/2$) above the SC, is given by¹⁶

$$j_\phi(\rho, z) = -\frac{cm\Phi_0}{2\pi\lambda^3} \int_0^\infty dq \exp(-ql) q^2 J_1(q\rho) C(q, z), \quad (\text{A2})$$

with

$$C(q, z) = \frac{k \cosh\left[k\left(\frac{d}{2} + z\right)\right] + q \sinh\left[k\left(\frac{d}{2} + z\right)\right]}{(k^2 + q^2) \sinh(kd) + 2kq \cosh(kd)}, \quad (\text{A3})$$

where $k = \sqrt{1 + q^2}$, $\rho = \sqrt{x^2 + y^2}$ with respect to the dipole, and $J_\nu(x)$ is the Bessel function.

The components of the vortex magnetic field outside the superconductor are given by¹⁹

$$h_{vz}(\rho, z) = \frac{L\Phi_0}{2\pi\lambda^2} \int_0^\infty \frac{dq q}{Q} J_0(q\rho) \exp[-q(|z| - d/2)], \quad (\text{A4})$$

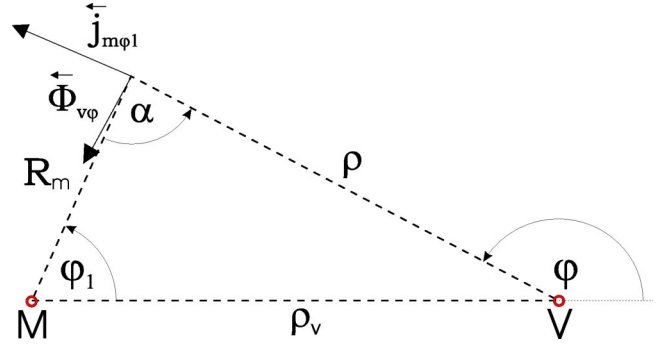


FIG. 11. Sketch of the system in the plane of the superconductor (xy plane). V and M denote the position of the vortex and the magnetic dipole, respectively.

$$h_{v\rho}(\rho, z) = \frac{L\Phi_0}{2\pi\lambda^2} \text{sgn}(z) \int_0^\infty \frac{dq q}{Q} J_1(q\rho) \exp[-q(|z| - d/2)], \quad (\text{A5})$$

where $Q = k[k + q \coth(kd/2\lambda)]$, ρ denotes the distance from the vortex, and $K_0(x)$ is the MacDonal function.

The first integral in Eq. (A1) now becomes (see Fig. 11 for definitions of the distance variables)

$$\begin{aligned} I_1 &= \frac{1}{2c} \int dV^{(i)} \vec{j}_m \cdot \vec{\Phi}_v \\ &= -\frac{m\Phi_0^2}{4\pi\lambda} \int_0^\infty dq \exp(-ql) q^2 \int_{-d/2}^{d/2} dz C(q, z) \int_0^{2\pi} d\phi \\ &\quad \times \int_0^\infty d\rho \rho J_1(qR) \frac{1}{2\pi\rho} \frac{\partial R_m}{\partial \rho}, \end{aligned}$$

where we make use of $\vec{j}_m \cdot \vec{\Phi}_v = j_{m\phi_1} \Phi_{v\phi} \cos \alpha = j_{m\phi_1} \Phi_{v\phi} (\partial R_m / \partial \rho)$.

$$\begin{aligned} I_1 &= \frac{m\Phi_0^2}{4\pi\lambda} \int_0^\infty dq C_1(q) \exp(-ql) q \frac{1}{2\pi} \\ &\quad \times \int_0^{2\pi} d\phi \int_0^\infty d\rho \frac{\partial(J_0(qR_m))}{\partial \rho} \\ &= \frac{m\Phi_0^2}{4\pi\lambda} \int_0^\infty dq C_1(q) \exp(-ql) q \frac{1}{2\pi} \int_0^\infty d\rho \frac{\partial}{\partial \rho} \\ &\quad \times \int_0^{2\pi} d\phi J_0(qR_m). \end{aligned}$$

Using Ref. 20 we obtain

$$\begin{aligned}
I_1 &= \frac{m\Phi_0^2}{4\pi\lambda} \int_0^\infty dq C_1(q) \exp(-ql) q \frac{1}{2\pi} 2\pi J_0(q\rho_v) \\
&\quad \times \int_0^\infty d\rho \frac{\partial(J_0(q\rho))}{\partial\rho} \\
&= -\frac{m\Phi_0^2}{4\pi\lambda} \int_0^\infty dq q C_1(q) \exp(-ql) J_0(q\rho_v), \quad (\text{A6})
\end{aligned}$$

where

$$C_1(q) = \frac{1}{k} \frac{k \sinh(kd) + q \cosh(kd) - q}{(k^2 + q^2) \sinh(kd) + 2kq \cosh(kd)}. \quad (\text{A7})$$

The integration of the second integral in Eq. (A1) gives

$$\begin{aligned}
I_2 &= -\frac{1}{2} \int dV^{(md)} \vec{h}_v \cdot \vec{M} = -\frac{1}{2} \int dV^{(md)} \vec{h}_{vz} \cdot \vec{M} \\
&= -\frac{m\Phi_0^2}{4\pi\lambda} \int_0^\infty \frac{dq q}{Q} \int_{-\infty}^\infty dz \delta(z-a) \exp[-q(|z|-d/2)] \\
&\quad \times \int_{-\infty}^\infty dy \delta(y-y_v) \int_{-\infty}^\infty dx \delta(x-x_v) J_0(q\sqrt{x^2+y^2}) \\
&= -\frac{m\Phi_0^2}{4\pi\lambda} \int_0^\infty \frac{dq q}{Q} \exp(-ql) J_0(q\rho_v). \quad (\text{A8})
\end{aligned}$$

After simple trigonometric transformations it can be shown that $C_1(q) = 1/Q$, and therefore from Eqs. (A6) and (A8) follows $I_1 = I_2$. We are allowed to generalize this equality for the case of finite size ferromagnets with out-of-plane magnetization, due to the superposition principle.

*Electronic address: peeters@uia.ua.ac.be

¹M. Baert, V.V. Metlushko, R. Jonckheere, V.V. Moshchalkov, and Y. Bruynseraede, Phys. Rev. Lett. **74**, 3269 (1995).

²J.I. Martin, M. Velez, J. Nogues, and I.K. Schuller, Phys. Rev. Lett. **79**, 1929 (1997).

³M.J. Van Bael, L. Van Look, K. Temst, M. Lange, J. Bekaert, G. Guentherodt, V.V. Moshchalkov, and Y. Bruynseraede, Physica C **332**, 12 (2000).

⁴M. Lange, M.J. Van Bael, L. Van Look, K. Temst, J. Swerts, G. Guentherodt, V.V. Moshchalkov, and Y. Bruynseraede, Europhys. Lett. **53**, 646 (2001).

⁵L.N. Bulaevskii, E.M. Chudnovsky, and M.P. Maley, Appl. Phys. Lett. **76**, 2594 (2000).

⁶I.F. Lyuksyutov and V.L. Pokrovsky, Phys. Rev. Lett. **81**, 2344 (1998).

⁷A.F. Kayali, Phys. Lett. A **298**, 432 (2002).

⁸S. Erdin, A.F. Kayali, I.F. Lyuksyutov, and V.L. Pokrovsky, Phys. Rev. B **66**, 014414 (2002).

⁹L.E. Helseth, Phys. Rev. B **66**, 104508 (2002).

¹⁰I.K. Marmoros, A. Matulis, and F.M. Peeters, Phys. Rev. B **53**, 2677 (1996).

¹¹Sa-Lin Cheng and H.A. Fertig, Phys. Rev. B **60**, 13 107 (1999).

¹²M.V. Milošević, S.V. Yampolskii, and F.M. Peeters, Phys. Rev. B **66**, 024515 (2002).

¹³D.J. Morgan and J.B. Ketterson, Phys. Rev. Lett. **80**, 3614 (1998).

¹⁴M.J. Van Bael, J. Bekaert, K. Temst, L. Van Look, V.V. Moshchalkov, Y. Bruynseraede, G.D. Howells, A.N. Grigorenko, S.J. Bending, and G. Borghs, Phys. Rev. Lett. **86**, 155 (2001).

¹⁵A.S. Mel'nikov, Yu.N. Nozdrin, I.D. Tokman, and P.P. Vysheslavtsev, Phys. Rev. B **58**, 11 672 (1998).

¹⁶M.V. Milošević, S.V. Yampolskii, and F.M. Peeters, Phys. Rev. B **66**, 174519 (2002).

¹⁷L.D. Landau and E.M. Lifshitz, *Theoretical Physics, Electrodynamics of Continuous Media* (Pergamon, Oxford, 1989).

¹⁸L.B. Ioffe and M.V. Feigelman, Phys. Rev. B **66**, 224503 (2002).

¹⁹M. Fusco-Girard and F. Mancini, Physica B & C **123**, 75 (1983).

²⁰I.S. Gradshteyn and I.M. Ryzhik, *Table of Integrals, Series, and Products* (Academic Press, London, 1994), p. 758, Eq. 6.684.